

# **Determination of Quantum Efficiency of UVIT Flight Model Detectors**

**C. S. Stalin, S. Sriram & Amit Kumar**

**Indian Institute of Astrophysics  
Bangalore 560 034**

**Version 0.1**

**17 December 2010**

## **1. Introduction**

UVIT has three FM detectors of same type for imaging in three wavelength regions FUV, NUV and VIS bands. During March 2010, some experiments were carried out at CREST, Hoskote, with an aim to calibrate the Quantum Efficiency (QE) of FM detectors of UVIT.

## **2. Calibration Tests on the Detectors:**

Calibration tests were carried out to measure the following

1. QE of the FUV detector
2. QE of the NUV detector
3. QE of the VIS detector

The QE measurement for each detector involves two steps

1. Measurement of the number of photons detected by the detector
2. Measurement of the total number of photons falling on the detector surface

Both these tests need the same experimental conditions to be maintained

### **3.0 Calibration of 3X3 holemask:**

To measure the total no. of photons falling on the detector input window, a NIST photo-diode was used. The sensitivity of NIST photo-diode is 1000 times lesser than that of the Flight Model Detector Modules (DM). Therefore, sufficient amount of light is to be made incident on the Photo-diode to get good results. However, if the same amount of light is allowed to incident on the FM DM it may damage the Detector. To avoid this damage a mask of hole size 500 microns and separation 5mm of 0.1% transmission was made to be placed in the collimated beam path for measuring the number of photons detected by the detector. However, before performing the experiment, the mask also needs to be well calibrated such that it is transmitting 0.1% of light incident on it.

### 3.1 Experimental Set-up:

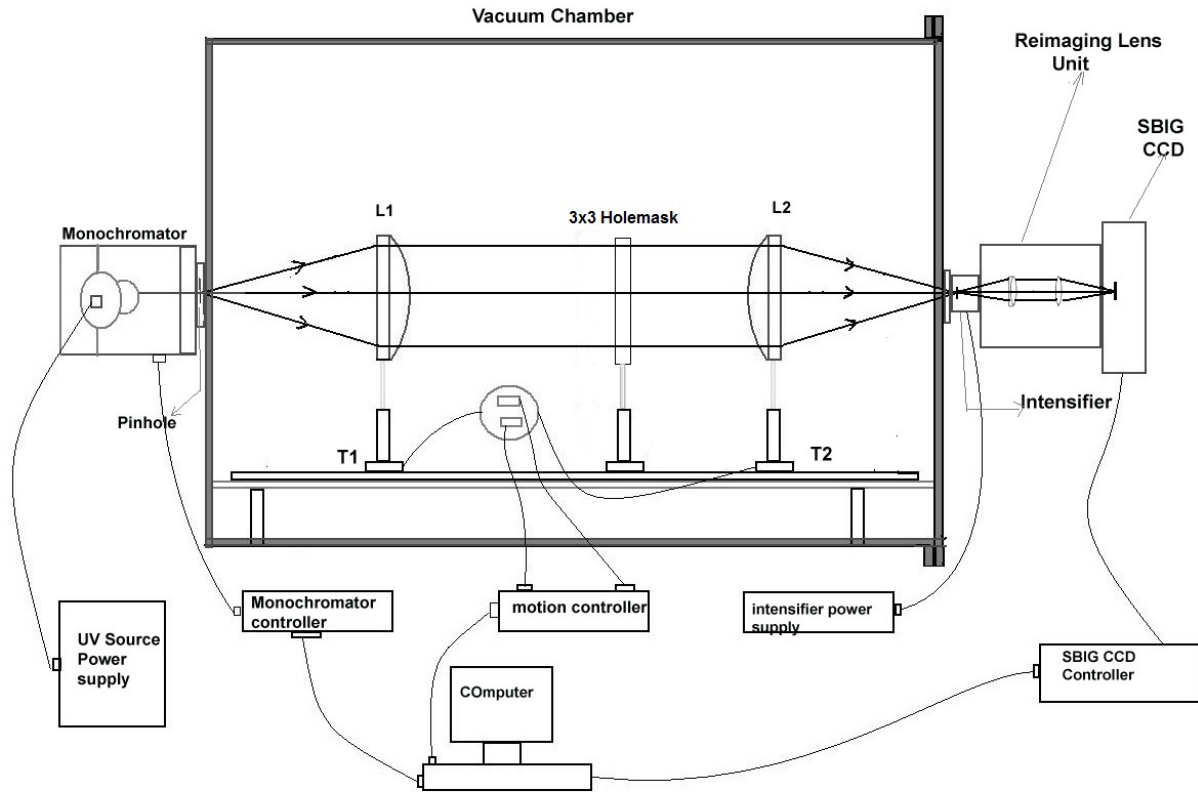


**Fig. 1:** Test set up for calibrating the mask

For calibrating the mask, the test set up as shown in Fig. 1 was used. Here, the input port of the vacuum chamber (evacuated to  $10^{-4}$  mbar) hosts the monochromator. This monochromator helps in selecting the desired wavelength. The light beam of any selected wavelength from the monochromator with an input slit width of 5 micron enters the vacuum chamber through a pinhole with a size of 50 micron. Diverging beam from the pinhole was made into a well collimated beam with the help of lens L1 placed at a certain distance from the aperture and is equal to the focal length of the lens. This collimated beam was focused on to the image intensifier mounted at the output port of the vacuum chamber with the help of another lens L2. The output beam from the image intensifier was focused onto a SBIG CCD camera with the help of re-imaging lens system. The positions of lenses L1 and L2 are adjustable as required for the wavelength, by moving the stages T1 and T2 with the help of the motion controller in order to get a well focused beam at the focal plane.

### 3.2 Data Acquisition & Analysis:

Three sets of data were acquired to determine the transmission of the mask.

#### Data Set 1:

First set of data was taken on 03/11/09. The experiment was done at four wavelengths namely, 182.3nm, 200.1nm, 213.8nm and 253.7nm. At each wavelength, the dark as well as light exposed frames were taken (five frames each) with and without mask. For image frames acquired without mask, the exposure time was 1 sec, whereas for image frames acquired with mask the exposure time was 20 secs. Each wavelength thus has five dark exposures and five light exposures. Median combine of the dark frames at corresponding wavelength for both open and mask image frames were done to prepare the master dark frame. Each light exposed frame was then subtracted by the corresponding master dark frame. For each wavelength, the set of five dark subtracted light exposed images were combined to get the final image to do photometry.

Here, as the image is not exactly circular, a polygon aperture was selected for the photometry. This photometry on polygon aperture was performed on images with and without mask for each of these five wavelengths.

The vertices of the polygon are (85,430), (235,430), (235,180),(85,180) and the center of polygon was at (160,305). For measuring the background, an annular ring having a width of 10 pixels was taken around the polygon. The results of the photometry after subtracting the background is given in Table 1.

**Table 1.** Mask calibration measurements for the data taken in 03/11/2009

Wave length in nm	Without mask		With mask		Counts/sec		Transmittance
	counts	Exp. time	counts	Exp. time	mask	open	
182.3	22565364	1s	121766	20s	60883.3	22565364	0.0027
200.1	19883880	1s	1018032	20s	50901.6	19883880	0.0026
213.8	22206482	1s	1740585	30s	58019.5	22206482	0.0026
253.7	69346272	5s	1164699	30s	38283.3	13869254	0.0028

#### Note:

Though the mask was designed to have a transmission of 0.1%, the results of the experiment done on 03/11/09 shows the transmission to be ~0.2%. This is because, the observed image was found to be out of focus.

### Data Set 2:

This data set was observed on 06/11/09, at the wavelengths 182.3nm, 187.9nm, 193.7nm, 200.3nm, 206.7nm, 213.8nm, 221.4nm, 229.6nm, 238.5nm and 253.7nm. At each wavelength image frames with and without mask were recorded. For open image frames, the exposure time was 5 sec, whereas for image frames with mask the exposure time was 30 sec. For photometry of the image frames, POLYPHOT available in IRAF was used.

The background counts were measured at four different positions on the image frame centered at (425,425); (425,125); (75,125); (325,125).with an annulus of 35.355 pixels and an annular width of 10 pixels. This is different from the procedure employed in the Data Set 1 to get the background. The average of the four background values at the four locations was taken as the mean background value for respective frame.

To measure actual image counts, a square box of width 250 pixels was fixed around the image location centered at coordinates (85,430); (335,430); (335,180); (85,180). The same polygon region was used for the photometry in both the frames acquired with and without the mask. A sample image frame with mask is shown in Fig. 2.

The results of the photometry are given in Table 2.

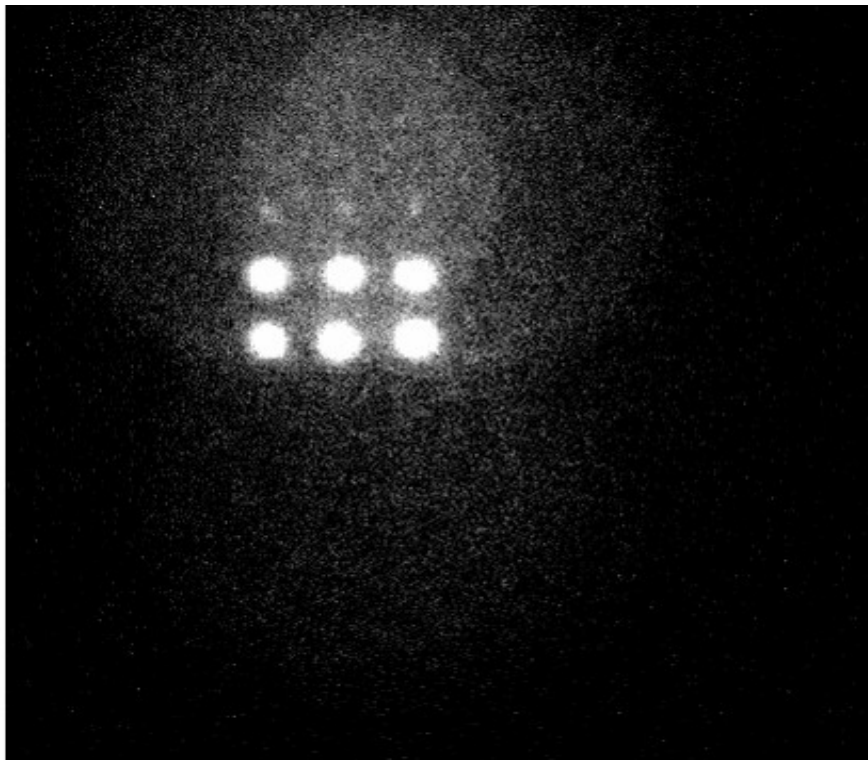


**Fig. 2.** Image of the hole mask on the SBIG Camera, with an exposure of 30 sec

**Table 2.** Mask calibration measurements for the data taken on 06/11/2009

Wave length in nm	Without mask		With mask		Counts/sec		Transmit.
	counts	Exp(s).	counts	Exp.(s)	Open	mask	
182.3	27501936	5	2229487	30	5500387	74316.2	0.0135
187.9	26733334	5	2210406	30	5346667	73680.2	0.0137
193.7	25677754	5	2148536	30	5135551	71617.8	0.0139
200.5	25494754	5	2192261	30	5098951	73075.3	0.0143
206.7	27241790	5	2161607	30	5448358	72053.5	0.0132
213.8	29008498	5	2092541	30	5801700	69751.3	0.012
221.4	28974226	5	2129399	30	5794845	70979.9	0.0122
229.6	28452938	5	2003260	30	5690588	66775.3	0.0117
238.5	27586428	5	2047449	30	5517286	68248.3	0.0123
253.7	23356226	5	1838867	30	4671245	61295.5	0.0131

**Note:**

The transmission of mask obtained here is different from expected value. This was because of the reflection of the light from the mask as can be seen in Fig. 2. The experiment was therefore repeated again.

**Data Set 3**

In a effort to get rid of the light reflection noticed in the Data Set 2 (a) the mask was coated with black (b) proper baffling was done to get rid of any external light and (c) the SBIG camera was covered with a black sheet. In addition to that, two more changes were made to the experimental set up described in Fig. 1 (a) the monochromator input slit was increased to 90 micron and (b) the monochromator output pin hole size was changed to 100 micron. These two changes were made based on the experiments done using the NIST photodiode. A sequence of 10 image frames of dark and light exposures were taken without mask in collimated beam path. The filter wheel was then rotated to select the 3x3 mask and again 10 image frames of light and dark were taken. This was repeated for 10 wavelengths. The exposure time of image frames with and without mask are 30 secs and 5 secs respectively. Dark frames were median combined to form master dark frames. These master dark frames were then subtracted from the corresponding light image frames. The dark subtracted light frames were then median combined to form one light frame each with and without mask for a total of 10 wavelengths. The number of counts in each final image with and without mask was estimated for each wavelength. The background counts estimated from few light free regions in the frame were subtracted from these counts. This was carried out with the CCD software which came along with the SBIG camera. An example image frame is shown in Fig. 3 . The light scattering seen in Fig. 2 is not seen here. The results of this experiment is given in Table. 3.



**Fig 3:** Image of the hole mask onto the SBIG Camera for an exposure of 30 seconds

**Table 3.** Mask calibration measurements for the data taken on 20/01/2010 (?)

Wave length in nm	Without mask		With mask		Counts/sec		Transmit. (%)
	counts	Exp (s).	counts	Exp. (s)	Open	mask	
182.3	198655916	5	1137172	30	39731183.2	37905.7	0.095
187.9	186332392	5	1056791	30	37266478.4	35226.4	0.095
193.7	171047802	5	968313	30	34209560.4	32277.1	0.094
200.5	164227076	5	933155	30	32845415.2	31105.2	0.095
206.7	165950556	5	947778	30	33190111.2	31592.6	0.095
213.8	167148703	5	949283	30	33429740.6	31642.8	0.095
221.4	161786796	5	902520	30	32357359.2	30084.0	0.093
229.6	154522655	5	848075	30	30904531.0	28269.2	0.091
238.5	146760649	5	809054	30	29352129.8	26968.5	0.092
253.7	123947176	5	712422	30	24789435.2	23747.4	0.096

The average transmittance = 0.095%

### 3.3 Measurement of the number of photons detected by the detector

#### Experimental setup:

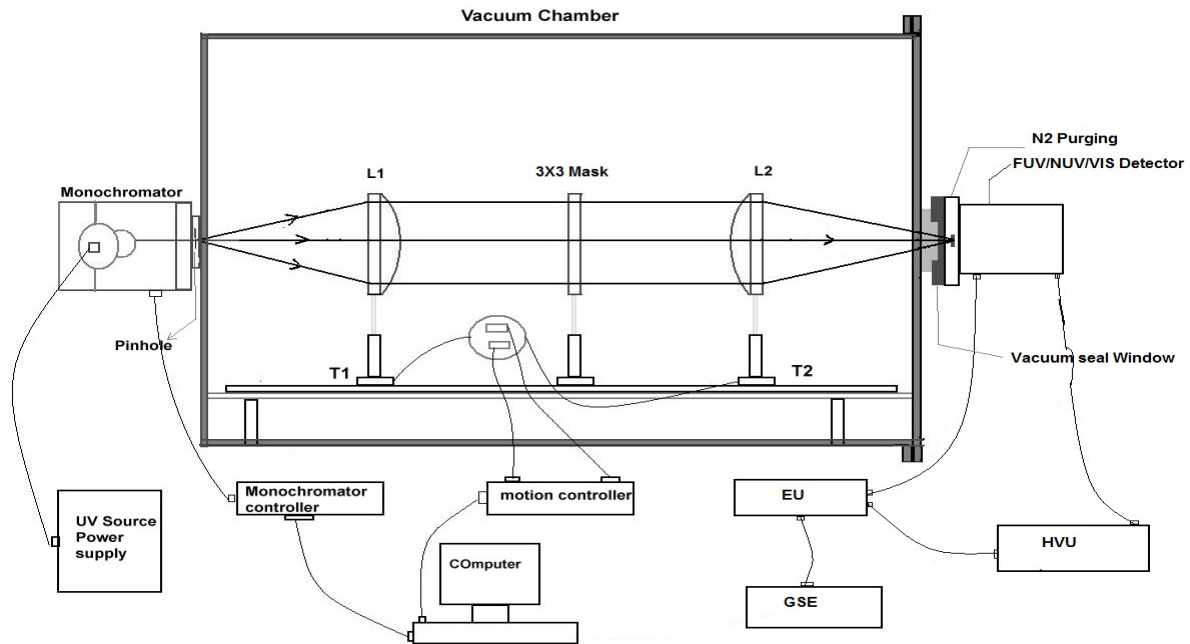


**Fig. 4. Test set up for measuring the QE**

The test setup for measuring the Q.E. is shown in Fig. 4. The input port of the vacuum chamber hosts the monochromator. Using the monochromator, the desired wavelength can be selected. The light beam of the selected wavelength from the monochromator with an input slit of 90 micron enters into the vacuum chamber through the monochromator output pinhole of size 100 microns. The diverging beam from the pinhole was made into a well collimated beam with the help of lens L1 placed at a certain distance from the pinhole, equal to the focal length of the lens. This collimated beam was then focused with the help of another lens L2 of same kind as L1 on to the photocathode inside the input window of FM detector module. The photocathode thus produces an electron for each incident photon. These photoelectrons were then accelerated through a gap of 100-200 mm towards the MCP stack resulting in an electron shower. At the rare end of the MCP stack, the electron shower

was fed through a fiber taper, the ends of which was fixed to the Star 250 CMOS image sensor. The positions of lenses L1 and L2 were adjustable as required for the wavelength, by moving the stages T1 and T2 with the help of the motion controller in order to get the well focused beam at the focal plane.

### **3.4 Data Acquisition:**

Using the experimental setup in Fig. 4, the images were acquired using the FM detectors.

#### **I. FUV DETECTOR:**

With FUV detector, the wavelength region 125 nm-155 nm was scanned. The complete detector was exposed (512X512pixels); however only 200X200 pixel region of the detector was read. The exposures were taken in photon counting mode and the images read with a frame rate of 172 frames/sec and the total exposure time in case of each wavelength was about 39 sec. While taking the exposures a 3x3 mask with 0.094% transmission was kept in the path of the light beam. The active area on the NIST photo-diode was 10 mm which corresponds to 3.3 mm area on the star250 CMOS sensor after fiber taper which is equivalent to 133x133 pixel area.

#### **II. NUV DETECTOR:**

With NUV detector, the wavelength region 170 nm-300 nm was scanned. The complete detector was exposed (512X512pixels); however only 200X200 pixel region of the detector was read. The exposures were taken in photon counting mode and the images read with a frame rate of 172 frames/sec and total exposure time in case of each wavelength was about 27 sec. While taking the exposures a 3x3 mask with 0.094% transmission was kept in the path of the light beam. The active area on the NIST photodiode is 10 mm which corresponds to 3.3 mm area on the star250 CMOS sensor after fiber taper and is equal to 133x133 pixel area.

#### **III. VIS DETECTOR:**

With VIS detector, the wavelength region 310 nm-550 nm was scanned. The complete

detector was exposed (512X512pixels); however only 200X200 pixel region of the detector was read. The exposures were taken in photon counting mode and the images read with a frame rate of 172 frames/sec and total exposure time in case of each wavelength was about 32 sec. While taking the exposures a 3x3 mask with 0.094% transmission was kept in the path of the light beam. The active area on the NIST photodiode is 10 mm which corresponds to 3.3 mm area on the star250 CMOS sensor after fiber taper and is equal to 133x133 pixel area.

### **3.5 Data Analysis:**

At each wavelength for the given exposure time the output data file was created in the .img format, which contains both science data and telemetry information. Each \*.img file is of size 512MB and it consist of many \*.raw (FITS) files. The conversion from \*.img to \*.raw was made by using the CCDLAB software developed at University of Calgary by Joe Postma. A set of three \*.fits files were first created from each \*.img file. Set 1 consists of (X-  $\Delta x$ ) frames, Set 2 consists of (X- ( $\Delta x+1000$ )) frames and Set 3 consists of (X- ( $\Delta x+2000$ )) frames. Here X refers to the total number of frames in one .img file and  $\Delta x$  refers to the number of frames in the Ramp time. Photometry was performed on these three .fits files.

#### **i. FUV region:**

Here the main objective was to determine total number of counts on the detector surface. In order to calculate the counts three concentric boxes of sizes 30x30 Pixels, 50x50 Pixels and 70x70 Pixels were considered. The three different regions were selected, because the background was found to be non-uniform across the image.

Photometry was done on these three apertures with help of POLYPHOT task in IRAF. To measure the background value a ring of 20 pixels width was fixed around the annulus of diameters 21.213 pixels, 35.355 pixels and 49.5 pixels respectively for the apertures of sizes 30x30 pixels, 50x50 pixels, 70x70 pixels. By running the POLYPHOT task, the total number of counts was obtained in the respective regions. The measured counts after background subtraction was then converted to counts/sec. The same procedure was repeated for all the wavelengths in the region.

#### **ii. NUV region & VIS region:**

The same procedure as detailed above for FUV was repeated in case of NUV and VIS regions as well and the counts per second was measured.

The above photometry resulted in the total number of photons detected by the FM detectors. To get the QE of the detectors, the total number of photons falling on the detector needs to be known. Therefore, to know the photons incident on the detector, another experiment was conducted using the NIST photo-diode.

### **3.6 Measurement of total number of photons incident on the detector**

The experimental setup remains almost the same as in Fig. 4, except two changes (i) the light was allowed to fall on the Photodiode mask without any mask in the path of the beam and (ii) NIST photo-diode was mounted on the output port of the detector chamber instead of FM-detectors. This is shown in Fig. 5. The output voltage of the NIST photodiode due to the incident photons was measured with the help of a multimeter connected to the photo-diode.

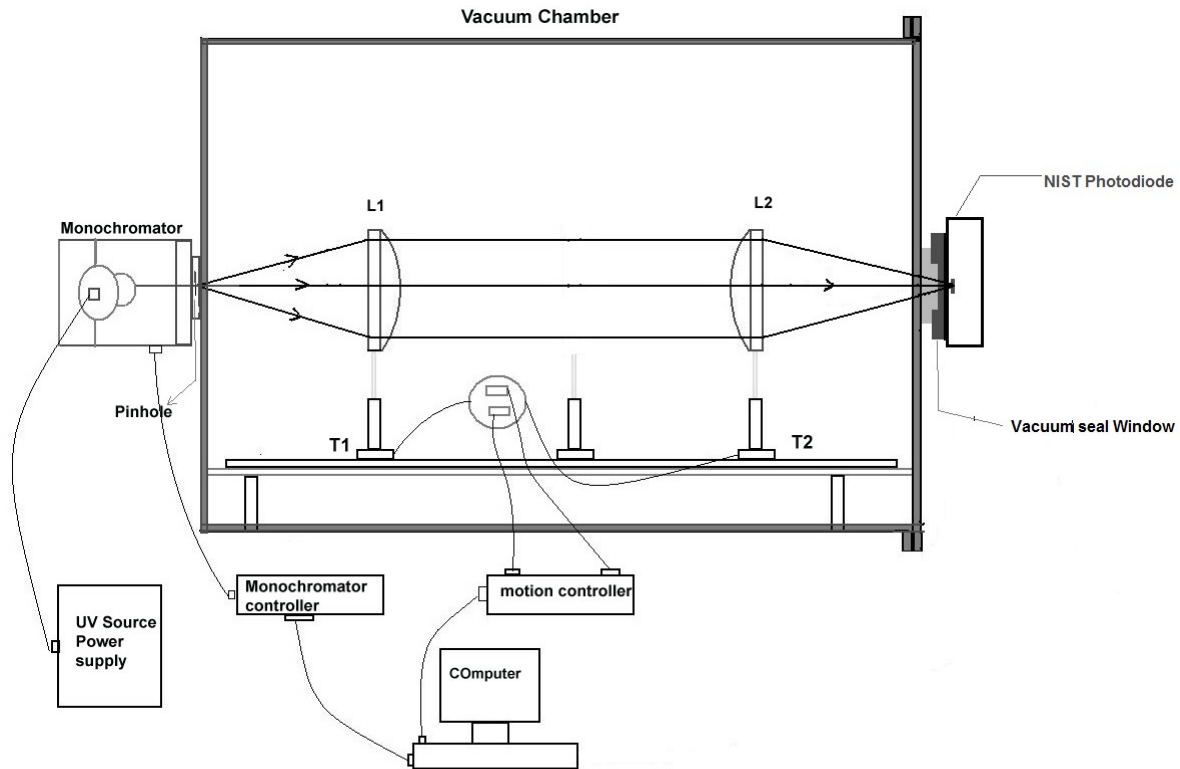


**Fig. 5.** Experimental set up for NIST photo-diode measurements

### 3.7. NIST Photo Diode:

International Radiation Detectors Silicon Photodiode AXUV 100G was used in the experiment for determining the absolute QE of the FM detectors. Using this test photodiode, the total number of photons falling on the detector window was measured (from the output voltage produced by the photodiode).

The test photodiode S/N 08-6 10, is a windowless International Radiation Detectors (IRD) AXUV 100G Silicon Photodiode supplied by the National Institute of Standards and Technology. The active area of the photodiode was approximately  $1 \text{ cm}^2$ . The spectral power responsivity for the region (200 nm-110 nm) was in the calibration report provided by the manufacturer and is used for further measurements with the detector.

### 3.8 Data Acquisition with NIST Photodiode:

The experimental set up shown in Fig. 5 was used to acquire data using the NIST photo-diode.

**i. FUV Region:**

In this region data was acquired in the wavelength region 125 nm-155 nm, (for the same wavelengths, which were used to acquire the exposures by the FUV detector).For each wavelength the photo-diode was exposed and the output current (voltage) of the photo-diode was fed to an amplifier circuit and the amplified output voltage of the diode was measured. For each wavelength, a set of 10 output voltages were measured with light exposure. For the same wavelength before exposing the diode to light, a set of ten output voltage values for dark exposure was also measured. The same procedure was repeated for all the remaining wavelengths in the region.

**ii. NUV Region:**

In this region data was acquired in the wavelength region 170 nm-300 nm, (for the same wavelengths, which were used to acquire the exposures by the NUV detector).For each wavelength the photo-diode was exposed and the output current (voltage) of the photo-diode was fed to an amplifier circuit and the amplified output voltage of the diode was measured. For each wavelength a set of 10 output voltages were measured with light exposure. For the same wavelength before exposing the diode to light, a set of ten output voltage values for dark exposure was also measured. The same procedure was repeated for all the remaining wavelengths in the region.

**iii. VIS Region:**

In this region data was acquired in the wavelength region 310 nm-550 nm, (for the same wavelengths, which were used to acquire the exposures by the VIS detector).For each wavelength the photo-diode was exposed and the output current (voltage) of the photo-diode was fed to an amplifier circuit and the amplified output voltage of the diode was measured. For each wavelength a set of 10 output voltages were measured with light exposure. For the same wavelength before exposing the diode to light, a set of ten output voltage values for dark exposure was also measured. The same procedure was repeated for all the remaining wavelengths in the region.

### 3.9. Data Analysis:

For each wavelength, a set of ten output voltages with light and dark exposures were obtained. From these ten output voltages the average was determined in case of both light as well as dark exposures. The difference between the voltage of light and dark exposures gives the resultant voltage due to the incident photons on the photo diode surface. This procedure was followed to measure the resultant voltage due to incident photons on the photo-diode surface for all wavelengths in the three regions (FUV, NUV, and VIS). From this measured resultant voltage, the number of photons incident on the surface of the photo diode was estimated by using the spectral responsivity of the photo-diode provided by the manufacturer.

The number of photons falling on the surface of the FM detector was obtained by multiplying the transmission of the mask (used in the path of the light while acquiring the images with FM detectors) and the photons falling on the photo-diode surface. Also we had a measure of the number of photons detected by the detector using the experimental set up shown in Fig. 4 using the procedures outlined in Section 3.3. The ratio between number of photons detected to the number of photons falling on the detector surface provides the QE of the detector. The same procedure was repeated for all wavelengths in FUV, NUV and VIS regions to measure the QE of all the three detectors.

### 4. Results:

The results of the QE measurements are given in Tables 4, 5 and 6 and in Figures 6, 7 and 8. As seen in the Figures 6, 7 and 8, the QE determined through three different box sizes match reasonably well in the case of FUV and NUV, however, little differences are noted in the case of VIS.

Wavelength in nm,	Avg. Q.E.			Standard Deviation		
	30x30	50x50	70x70	30x30	50x50	70x70
125.4	4.3802	6.0467	6.2213	0.0074	0.0154	0.0196

135.4	4.6816	4.8383	4.8984	0.005	0.0065	0.01
140.3	4.4136	4.5259	4.5694	0.0007	0.0013	0.0008
144.1	3.8911	3.9961	4.0389	0.0051	0.005	0.0056
148.7	3.5785	3.6701	3.7067	0.0046	0.0043	0.0044
154.5	3.3568	3.4497	3.4836	0.0015	0.0013	0.0028
160.8	2.682	2.7342	2.7594	0.0025	0.0027	0.0028
164.8	2.7088	2.7715	2.7992	0.0044	0.0042	0.0038
170	2.3833	2.4402	2.4671	0.0012	0.0022	0.0016
175	1.6253	1.669	1.6884	0.0037	0.0041	0.005
182.3	0.4062	0.4173	0.425	0.0032	0.0037	0.004

**Table 4.:** FM-FUV Detector Module Quantum Efficiency

Wavele ngth in nm	Avg. Q.E.(3sets)			Standard Deviation		
	30x30	50x50	70x70	30x30	50x50	70x70
170	5.6335	6.1826	6.4206	0.0092	0.0063	0.0077
175	7.1195	7.619	7.7712	0.0088	0.0093	0.0098
182.3	7.8746	8.2369	8.3685	0.0017	0.0018	0.0020
187.9	8.3675	8.7251	8.8653	0.0054	0.0061	0.0064
193.7	8.8071	9.1749	9.3574	0.0022	0.0018	0.0011
200	8.8311	9.2068	9.4093	0.0056	0.0061	0.0057
206.7	9.0837	9.5096	9.7329	0.0096	0.0084	0.0078
213.8	9.3641	9.8063	10.057	0.0066	0.0065	0.0076
221.4	9.7502	10.254	10.533	0.0049	0.0060	0.0054
229.6	10.012	10.573	10.905	0.0666	0.0028	0.0041
238.5	9.6002	10.18	10.541	0.0900	0.0144	0.0186

253.7	8.8302	9.4074	9.859	0.0140	0.0175	0.0179	
255	8.7606	9.3339	9.7605	0.0055	0.0058	0.0046	
260	8.3608	8.9232	9.3512	0.0087	0.0092	0.0082	
265	7.4982	8.0081	8.4006	0.0089	0.0058	0.0061	
270	6.8715	7.3665	7.7586	0.0133	0.0127	0.0129	
275	5.5574	5.985	6.3529	0.0117	0.0127	0.0090	
280	4.7527	5.1486	5.4916	0.0155	0.0136	0.0153	
285	3.6787	3.9887	4.2767	0.0099	0.0079	0.0048	
290	2.6332	2.8853	3.1287	0.0095	0.0097	0.0073	
295	1.7384	1.9389	2.1510	0.0031	0.0005	0.0035	
300	1.0655	1.2217	1.3896	0.0020	0.0019	0.0038	
305	0.7573	0.863	1.0181	0.0033	0.0055	0.0054	

**Table 5.:** FM-NUV Detector Module Quantum Efficiency

Wavelength in nm	Avg. Q.E			Standard Deviation		
	30*30	50*50	70*70	30*30	50*50	70*70
	310	9.18729	10.0555	10.4061	0.02434	0.212
315	9.43109	10.3241	10.7312	0.02259	0.23925	0.01219
325	7.75047	8.48262	8.87785	0.03211	0.02886	0.34638
335	7.99422	8.98052	9.27747	0.03124	0.05363	0.40836
345	8.56115	9.78163	10.1584	0.05738	0.03262	0.52722
355	8.97141	10.0771	10.293	0.05781	0.04986	0.08527
365	8.85818	9.57204	10.2848	0.10511	0.22224	0.06206
375	8.82711	9.59647	10.4502	0.12306	0.27612	0.07
385	9.06981	9.7753	10.7538	0.00531	0.07135	0.06818
395	8.90267	10.459	11.0523	0.02509	0.17668	0.16553
405	8.59783	10.3116	11.0308	0.02271	0.2335	0.19422

415	8.3459	10.0684	10.8773	0.07652	0.24485	0.22446	
425	8.93378	10.9754	11.7654	0.05799	0.30119	0.21578	
435	8.27176	10.1176	11.3127	0.06268	0.302	0.20242	
445	8.51103	10.4376	11.5816	0.08764	0.31269	0.23584	
455	7.59153	9.88476	10.9946	0.11427	0.39428	0.26765	
465	7.62145	9.71655	10.8957	0.21853	0.36241	0.23423	
475	7.21219	9.48105	10.7739	0.20944	0.42108	0.24611	
485	6.82302	9.26469	10.1041	0.14069	0.2685	0.39272	
495	5.86352	8.28373	9.33401	0.1875	0.18838	0.25935	
505	5.4987	7.61171	8.60242	0.21693	0.17222	0.24338	
515	4.17115	5.9679	7.9761	0.71207	1.61889	0.14685	
525	5.05233	7.85536	9.78789	0.72192	0.05731	0.11301	
535	3.93402	5.93522	7.2725	0.53391	0.09618	0.11409	
545	3.59739	4.90946	6.29355	0.48781	1.12349	0.0722	
550	3.27207	4.89457	6.58397	0.66769	1.43018	0.02403	

**Table 6:** FM-Visual Detector Module Quantum Efficiency

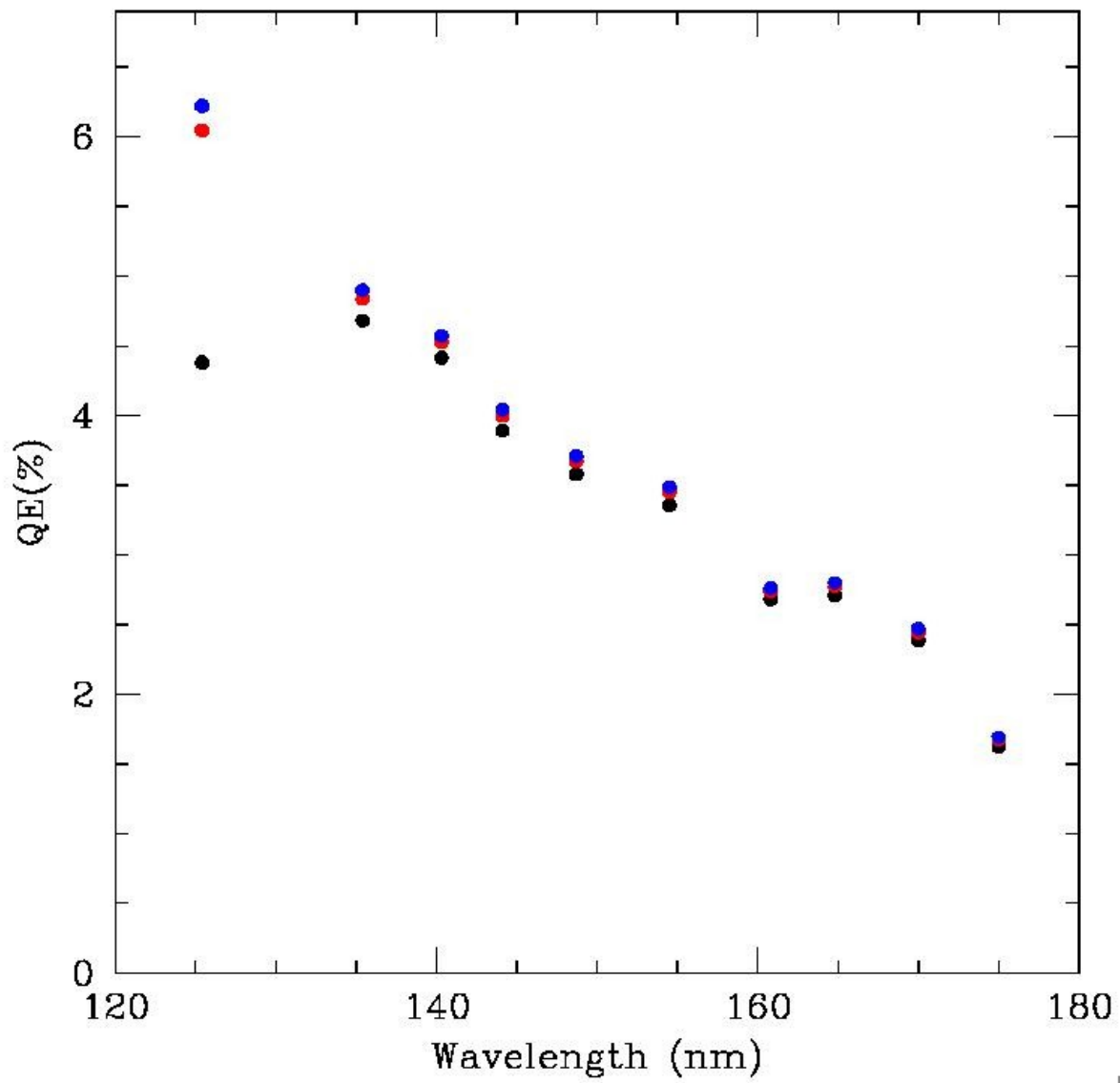


**Fig. 6:** QE of the FM FUV detector. Here black dots refers to the 30x30 region, red refers to the 50x50 region and blue refers to the 70x70 region.

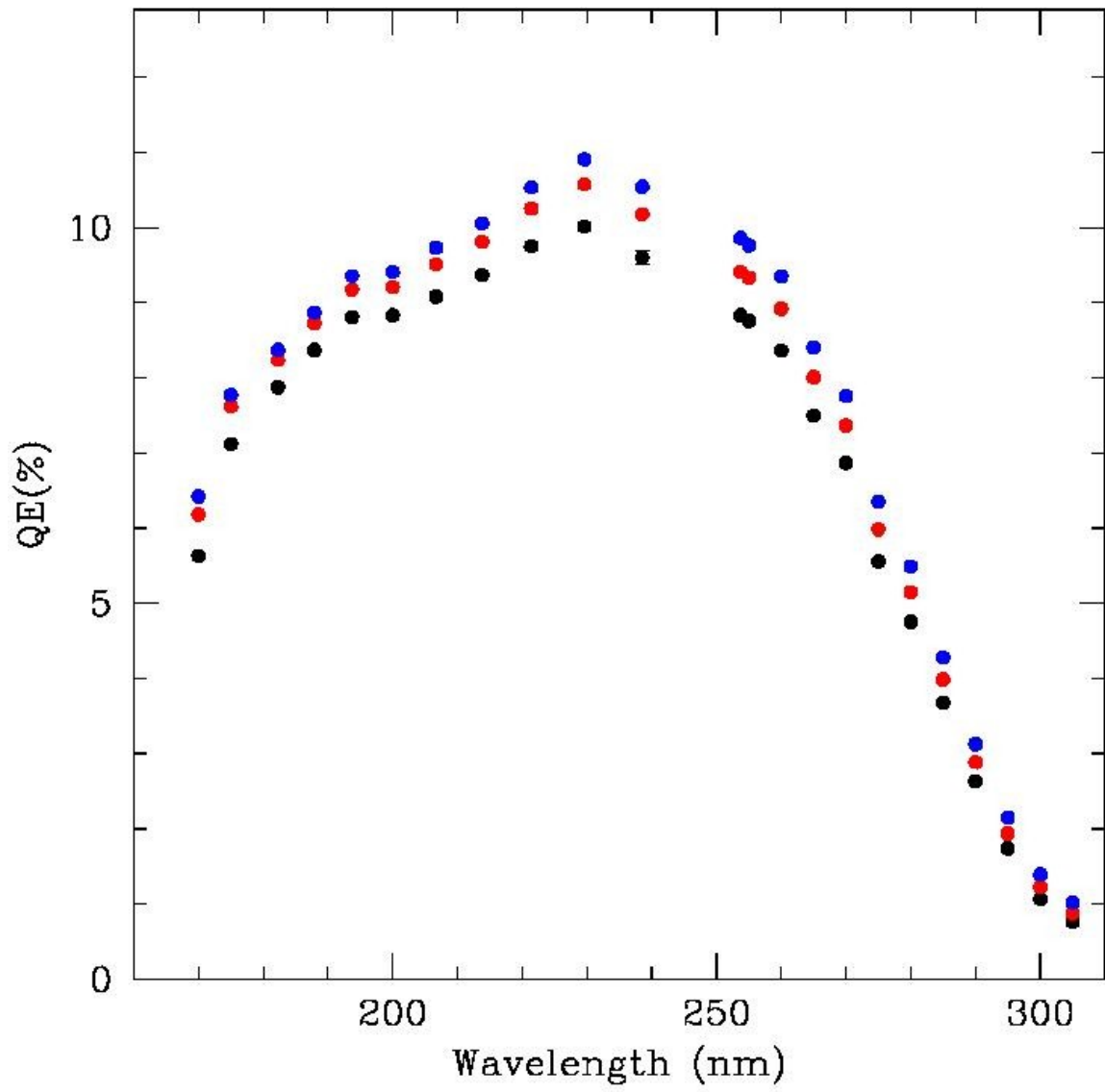
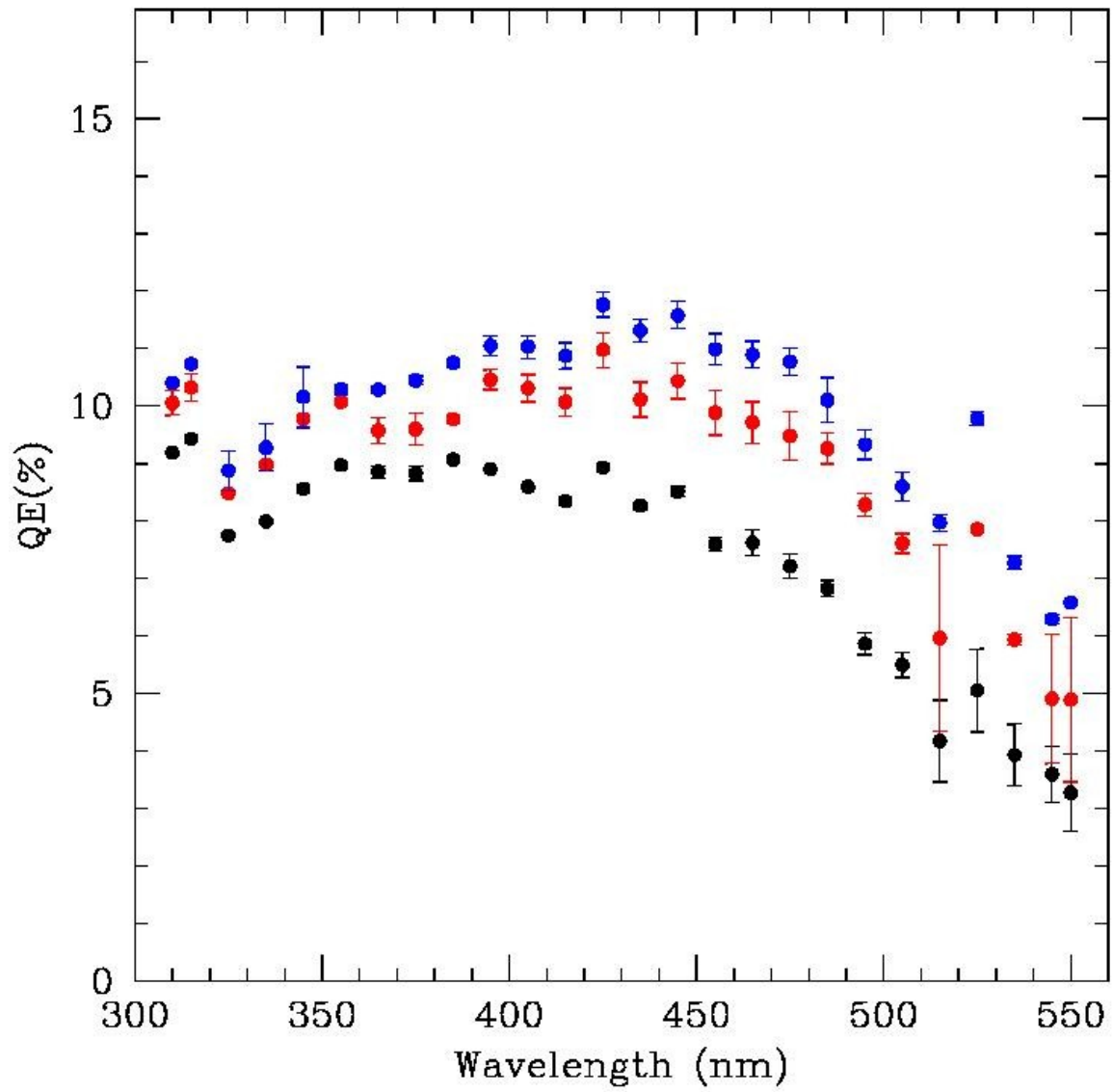


**Fig. 7.** QE of the FM NUV detector. Here black dots refers to the 30x30 region, red refers to the 50x50 region and blue refers to the 70x70 region.

**Fig. 8:** QE of the FM Visual detector. Here black dots refers to the 30x30 region, red refers to the 50x50 region and blue refers to the 70x70 region.



### Acknowledgement:

We thank Joe Postma for the NIST diode and his CCDLAB software. Also his help in CREST on taking the image exposures is thankfully acknowledged.